

CHAPTER 7 INTERPRETATION OF RESULTS OF NUMERICAL ANALYSES

The findings obtained in Chapter 6 are analyzed further in this chapter. This chapter shows the interpretation of the results divided into four sections.

7.1 Ground Acceleration

One of the findings explained in Chapter 6 is that the input ground acceleration (p_{ga}) is de-amplified for cases with Loma Prieta earthquake and is amplified for cases with Saguenay earthquake except for cases with silty sand layer underlain by soft clay, namely Cases 5S and 6S (refer to Section 6.3.4 and Table 6.16). To investigate this matter further, the values of p_{ga} and a_{max} obtained from FLAC analyses were plotted and compared to the plot of amplification ratios proposed by Seed and Idriss (1982) as shown on Figures 7.1 and 7.2.

Figure 7.1 shows plot of amplification ratios based on the soil type. As explained previously, the models analyzed using FLAC consist of three types of soil, that is silty sand, silty sand underlain by soft clay, and silt. Note that the two data points in the middle were obtained from Cases 1C2 and 2C2 using p_{ga} of 0.2g. Based on soil classification proposed by Seed and Idriss (1982), the three soil types used in this research would be classified as stiff soils. If the curve for stiff soils is used to estimate the value of a_{max} , it is apparent that this curve generally overestimates the values of a_{max} obtained from FLAC analyses. Note that Seed and Idriss (1982) developed the curves shown on Figure 7.1 based on earthquakes data from Western United States (WUS).

Figure 7.2 shows plot of amplification ratios in a slightly different way based on the ground condition: with or without aggregate pier. It is apparent that the use of aggregate pier amplifies the ground acceleration (a_{max}) by a factor ranging from 1.55 to 3.13 for Loma Prieta earthquake and 1.04 to 1.67 for Saguenay earthquake. The average value for both earthquake ranges from 1.4 to 2.3. This phenomenon is not completely surprising and has been shown by other researchers, for example by Liu and Dobry (1997) and Mitchell, et al. (1998). Liu and

Dobry (1997) studied a model of footing and showed that the amplification ratios of the footing resting on compacted sand zone within a liquefiable soil mass increase as the depth of the compacted zone increases.

The contrary conclusion, that is de-amplification for cases with Loma Prieta earthquake and amplification for cases with Saguenay earthquake, may be caused by two factors: the narrow and short models used in FLAC analyses (8.4 feet by 14.5 feet or 26.5 feet) and the huge difference in pga values (0.45g and 0.05g for Loma Prieta and Saguenay earthquakes, respectively) caused the models to give different response.

As noted previously in Section 5.3, the Fourier amplitude spectrum expresses the frequency content very clearly. Therefore, it is necessary to investigate the frequency content of ground acceleration (a_{\max}) of each cases analyzed using FLAC and compare them to the input ground acceleration (pga).

Figures 7.3 and 7.4 show the Fourier amplitude spectra for cases using Loma Prieta and Saguenay earthquake, respectively. Note that the scale for the abscissa (frequency) is in logarithmic scale. The Fourier amplitude spectra for the peak acceleration on rock outcrops (pga) are presented in black lines while the spectra for the peak acceleration at the soil surface (a_{\max}) are presented in gray lines.

Tables 7.1 and 7.2 summarize the frequency at which the maximum acceleration values (pga or a_{\max}) occur. It can be concluded that for Loma Prieta earthquake the frequency of pga coincides with the frequencies of a_{\max} . For Saguenay earthquake the frequency of pga is slightly larger than the frequencies of a_{\max} . It can also be concluded that cases using Loma Prieta earthquake generally show spectra with low frequency (high period) while cases using Saguenay earthquake generally show spectra with high frequency (low period).

7.2 Excess Pore Water Pressure Ratio

The second parameter that will be discussed in this section is the excess pore water pressure ratio (r_u). Both the peak and the steady state values of r_u were collected and compared between cases with and without aggregate pier to observe whether or not improvement occurs by installing aggregate pier. Figure 7.5 shows the plot of peak r_u values for cases without

aggregate pier versus peak r_u values for cases with aggregate pier both for Loma Prieta and Saguenay earthquakes. The individual plot for each earthquake is presented on Figures 7.6 and 7.7 for Loma Prieta and Saguenay earthquakes, respectively. A best-fit curve was plotted for each figure.

From Figure 7.6 it is apparent that most of the data points actually lay above the 1:1 line that is the dashed line. It means that for Loma Prieta earthquake most r_u values are increased due to the installation of aggregate pier.

Figure 7.7 shows that for Saguenay earthquake most of the data points lay beneath the 1:1 line (the dashed line). It means that for Saguenay earthquake most r_u values are decreased due to the installation of aggregate pier.

Since Figure 7.5 shows that most data points lie beneath the 1:1 line, it can be concluded that generally improvement occurs due to the installation of aggregate pier.

Figures 7.8 to 7.10 show similar plots to those of Figures 7.5 to 7.7 but for the steady state r_u values for both earthquakes, for Loma Prieta earthquake, and for Saguenay earthquake, respectively. All the three plots show that most of the data points lay beneath the 1:1 line (the dashed line). It can be concluded that generally improvement occurs due to the installation of aggregate pier.

As noted previously, factor of safety against liquefaction (FS_L) can be calculated based on the Simplified Procedure (Seed and Idriss, 1971) as explained in Section 3.1. For values of FS_L equal or larger than unity, the residual excess pore water pressure ratio can be calculated using the method proposed by Marcuson, et al. (1990) as explained in Section 2.1.6.

Therefore, the procedure explained in the previous paragraph was performed only for cases with silty sand and with values of FS_L greater than unity, which only left Cases 1S and 3S. The r_u values obtained from Marcuson, et al. (1990) were compared with those from FLAC. Table 7.3 and Figures 7.11 and 7.12 show the comparison. Note that the r_u values from FLAC are the steady state values.

Figure 7.11 shows that the steady state r_u values calculated using Marcuson, et al. (1990) procedure underestimate those calculated using FLAC for Case 1S. It is apparent that the r_u values from FLAC decrease with depth while the Marcuson, et al. (1990) procedure gives relatively constant values with depth. The relatively constant values were caused by the high values of factor of safety against liquefaction (FS_L) predicted using the Simplified Procedure

(Seed and Idriss, 1971) as shown on Table 7.3. Marcuson, et al. (1990) showed that the rate of change of the residual excess pore water pressure ratio is less significant for high values of FS_L as shown on Figure 2.6.

Figure 7.12 shows that similar conclusion to that of Case 1S can be drawn for Case 3S. The values of r_u decrease with depth with less significant decrease in r_u values beyond depth of about 17 feet.

It can be concluded that the residual (steady state) r_u values calculated using Marcuson, et al. (1990) procedure underestimate those calculated using FLAC.

7.3 The Shear Stress Reduction Factor

The following section will focus the discussion on the shear stresses in the soil matrix whose analyses were previously discussed in Section 6.4.

As explained previously in Chapter 3, in the Simplified Procedure proposed by Seed and Idriss (1971) the maximum shear stress in soil matrix (τ_{max}) can be estimated by multiplying the stress reduction coefficient (r_d), total overburden pressure (σ_0), and the peak horizontal acceleration at the ground surface (a_{max}) as shown in equation (3.5). By using the values of maximum shear stresses (τ_{max}) obtained from FLAC analyses, the stress reduction coefficient (r_d) can be calculated and compared to the values proposed by Seed and Idriss (1971).

$$r_d = \frac{\tau_{max}}{\sigma_0 * \frac{a_{max}}{g}} \quad (7.1)$$

The procedure outlined above was performed for both cases with and without aggregate pier (Cases 1C2 and 2C2, respectively) for the soil matrix.

By using equation (7.1), the stress reduction coefficient (r_d) can be calculated as shown on Figure 7.13. The average values for Case 1C2 are shown by dashed line and those of Case 2C2 are shown in solid line. The r_d values for Case 1C2 decrease with depths up to depth of

about 2 feet and then increase with depths. For Case 2C2, the r_d values decrease quickly at depths close to the ground surface and then remain relatively constant and increase quickly again. It is apparent that the r_d values for Case 1C2 (without aggregate pier) are generally larger than those of Case 2C2 (with aggregate pier) except for depths close to the ground surface. From Figure 7.13 it can be concluded that the values of r_d calculated using FLAC are generally less than those proposed by the Simplified Procedure (Seed and Idriss, 1971).

The conclusion drawn in the previous paragraph for Cases 1C2 and 2C2 seems contrary to intuition. The r_d values for case with aggregate pier are supposed to be larger than those for case without aggregate pier, which means more reduction in the shear stress in the soil matrix due to installation of aggregate pier because the aggregate pier will carry more shear stresses than the soil matrix. Two factors contributed to this contradiction. First, both cases have different values of a_{max} : 0.138g and 0.366g for Cases 1C2 and 2C2, respectively. It is apparent that the difference in a_{max} values will affect the calculation of r_d values as shown in equation (7.1). Second, the time at which the maximum shear stress (τ_{max}) occurs in the shear stress time histories is different for each case: 0.615 second for Case 1C2 and 1.079 seconds for Case 2C2. The time was selected as the time at which the maximum shear stress (τ_{max}) occurs at the middle grid of the model analyzed using FLAC. This was done because the value of a_{max} was taken in the middle gridpoint. Once this time was determined, all of the maximum shear stress (τ_{max}) values for other elements were read at the same corresponding time. However, both cases were still compared to each other because the same earthquake record was used that is the Loma Prieta earthquake record.

Baez and Martin (1993, 1994) and Goughnour and Pestana (1998) introduced a new parameter, which they defined as the shear stress reduction factor (K_G) as previously discussed in Chapter 3. Equations (3.24) and (3.31) show the determination of K_G values. The shear stress in soil matrix can be estimated by multiplying K_G with the average shear stress (τ_{ave}) calculated using equation (3.6) as proposed in the Simplified Procedure (Seed and Idriss, 1971). Equation (3.6) can be written in terms of maximum shear stress (τ_{max}):

$$\tau_{max} = \sigma_0 * \frac{a_{max}}{g} * r_d \quad (7.2)$$

Hence, equation (3.24) can also be written in terms of maximum shear stress (τ_{\max}).

$$K_G = \frac{\tau_s}{\sigma_0 \frac{a_{\max}}{g} r_d} \quad (7.3)$$

By applying values of τ_{\max} calculated using FLAC into equation (7.3), the values of K_G can be calculated. This procedure was applied to the case with aggregate pier (Case 2C2) with value of a_{\max} of 0.366g. Figure 7.14 shows plot of K_G values versus distance for different depths. The values of K_G vary between close to zero and 0.7 in the soil matrix and between 0.1 and 2 in the aggregate pier. It is apparent that the K_G values in the aggregate pier (bound by the vertical lines) are larger than those in the soil matrix. This shows that the installation of aggregate pier is effective in that the aggregate pier carries more shear stresses than the soil matrix under seismic loading.

The average of K_G values shown on Figure 7.14 is shown on Figure 7.15. It can be seen that the values of $(K_G)_{\text{ave}}$ vary between 0.1 and 0.3 in the soil matrix and between 0.24 and 1.34 in the aggregate pier.

Figure 7.16 shows Figure 7.15 in a slightly different way that is the average values of K_G were plotted against depths. It decreases with depth up to about 3 feet and then remains relatively constant and then increases again at about 11 feet. It can be seen that the average value of K_G is 0.17 throughout all depths.

The values of K_G calculated using equation (7.3) were based on shear stress calculated using the Simplified Procedure (Seed and Idriss, 1971), which does not take into account the effects of reinforcing elements. To overcome this problem a modification to the shear stress reduction factor (K_G) is introduced that is the shear stress reduction factor, which takes into account the reinforcement factor (K_{GR}). The value of K_{GR} is nothing more than the ratio of the maximum shear stress for case with aggregate pier to that of case without aggregate pier obtained from FLAC analyses.

$$K_{GR} = \frac{(\tau_{\max})_{\text{with aggregate pier}}}{(\tau_{\max})_{\text{without aggregate pier}}} \quad (7.4)$$

To make the discussion easier, the case analyzed was given a new name that is Case C2 that represents the ratio of Case 2C2 and Case 1C2 in equation (7.4). Figures 7.17 to 7.19 show the results for Case C2.

Figure 7.17 shows plot of K_{GR} values versus distance for different depths. The values of K_{GR} vary between close to zero and 2.8 in the soil matrix and between 0.3 and 19.5 in the aggregate pier. It is apparent that the K_{GR} values in the aggregate pier (bound by the vertical lines) are much larger than those in the soil matrix. This again shows that the aggregate pier carries more shear stresses than the soil matrix under seismic loading.

The average of K_{GR} values shown on Figure 7.17 is shown on Figure 7.18. It can be seen that the values of $(K_{GR})_{ave}$ vary between 0.3 and 1.2 in the soil matrix and between 0.9 and 9.9 in the aggregate pier.

Figure 7.19 shows Figure 7.18 in a slightly different way that is the average values of K_{GR} were plotted against depths both for soil matrix and aggregate pier. The trend of this plot is similar to that of K_G values. For the soil matrix, it increases at depths close to the ground surface and then decreases up to about 3 feet and then remains relatively constant and then increases again at about 10 feet. From Figure 7.19, it can be seen that the values of K_{GR} are approximately 0.6 and 3.6 for the soil matrix and the aggregate pier, respectively.

It can be concluded that the average value of K_{GR} for soil matrix (0.6) is much larger than the value of K_G of 0.17 for Case 2C2. It is apparent that the value of K_G calculated using equation (7.3) gives smaller value than the value of K_{GR} calculated using equation (7.4). The use of K_{GR} value is more preferable since it depicts the “real” reinforcing effects of aggregate pier as shown in equation (7.4).

The values of K_G shown on Figure 7.16 were compared to the values of K_{GR} shown on Figure 7.19 in Figure 7.20 for different depths. In other words, Figure 7.20 shows the comparison of the values of K_{GR} calculated using equation (7.4) and the values of K_G calculated using equation (7.3) for Case C2. A trend line is also shown on this figure. It can be concluded that the use of K_G based on shear stresses from FLAC normalized by those from the Simplified Procedure overestimates the reduction in shear stress of soil matrix during seismic loading compared to the use of K_{GR} .

A general procedure should be developed to estimate the value of K_{GR} . For this purpose, the procedures proposed by Baez and Martin (1993, 1994) and Goughnour and Pestana (1998) were reviewed.

In FLAC analyses, the effect of composite material was included (refer to Section 5.1.2). On the contrary, it is usually neglected in practice. Therefore, the shear modulus (G) of the aggregate pier was calculated using equation (5.5) with elastic modulus (E) of 2,520,000 psf (eight times to that of soil matrix) and Poisson's ratio (ν) of 0.2 (refer to Table 5.1). Hence, a shear modulus (G) value of 1,058,824 psf was obtained. Table 5.1 shows that the shear modulus (G) of soil matrix is equal to 118,125 psf. Hence, shear modulus ratio (G_r) of 8.96 should be obtained. Using this value, a value of K_G of 0.6 was obtained for area replacement ratio (A_r) of 10% calculated using equation (3.24) as proposed by Baez and Martin (1993, 1994). If the procedure proposed by Goughnour and Pestana (1998) is used, a value of K_G of 0.8 was obtained by using equation (3.31).

It can be concluded that the value of K_G calculated using equation (3.24) as proposed by Baez and Martin (1993, 1994) gives the same value as the value of K_{GR} calculated using equation (7.4). Therefore, equation (3.24) can be used in designing the reinforcing effects of aggregate pier foundation system during seismic loading.

Figure 7.21 presents equation (3.24) in form of a chart. It is apparent that at any given A_r , the reinforcement factor (K_{GR}) decreases with increasing shear modulus ratio (G_r). It can also be seen that at any given R_s , the reinforcement factor (K_{GR}) decreases with increasing area replacement ratio (A_r).

7.4 Implications for Design of Aggregate Pier under Seismic Loading

The major findings explained in the previous sections give implications in the design of aggregate piers under seismic loading. The following procedure can be used to determine the magnitude of the shear stress in soil matrix (τ_s) due to seismic loading:

1. Estimate the peak horizontal acceleration on ground surface (a_{max})
2. Estimate the input shear stress (τ) using equation (3.5)

3. Calculate the value of K_{GR} using equation (3.24)
4. Calculate the shear stress in soil matrix (τ_s) as

$$\tau_s = K_{GR} * \tau \quad (7.5)$$

where τ is calculated from step 2 using equation (3.5).

The value of a_{max} for liquefaction analyses can be estimated using the following methods, in order of preference (Youd, et al, 2001):

1. Empirical correlations of a_{max} with earthquake magnitude, distance from seismic source, and local soil condition (for example, Idriss, 1991),
2. Local site response analyses using computer code, such as SHAKE and DESRA (Schnable, et al, 1972; Finn, et al, 1977), or
3. Amplification ratios, for example such as the one proposed by Idriss (1990, 1991).

Figure 7.22 shows the application of the procedure outlined above for Case 2C2 (case with aggregate pier). The value of a_{max} used in this case is the one calculated from FLAC ($a_{max} = 0.366g$). Figure 7.22 also shows the values of τ_{max} versus depths at different distance calculated using FLAC. It is apparent that the use of τ_{max} calculated by equation (3.5) gives conservative values in estimating τ_s as shown by the thick solid line. Hence, a reduction factor should be applied in estimating the values of the input shear stress (τ).

For Case 2C2, it is suggested to use a correction factor of 0.65, i.e. use the value of average shear stress (τ_{ave}) calculated using equation (3.6) in step 2 in the procedure mentioned above instead of using the maximum input shear stress (τ_{max}) calculated using equation (3.5). The values of τ_s using τ_{ave} as the input shear stress are shown in dashed lines on Figure 7.22.

The following aspects should be considered carefully in designing the aggregate pier under seismic loading:

- As noted previously, the installation of aggregate pier shows improvement in terms of excess pore water pressure ratio (r_u). But it was also found that the installation of

aggregate pier amplifies the peak acceleration at the ground surface (a_{\max}). Both aspects should be taken into consideration in design.

- It is not recommended to use the procedure proposed by Marcuson, et al. (1990) to calculate the values of r_u based on the factor of safety against liquefaction (FS_L) calculated using the Simplified Procedure (Seed and Idriss, 1971). Marcuson, et al. (1990) procedure underestimates the r_u values calculated by using FLAC.
- The results from FLAC analyses seem contradict with those from the Simplified Procedure (Seed and Idriss, 1971) in terms of estimating the values of r_d and K_G . It is recommended to use the values of K_{GR} estimated using equation proposed by Baez and Martin (1993, 1994).
- A simple design procedure was proposed to estimate the shear stress in the soil matrix (τ_s) under seismic loading. This procedure should be used with judgment as to which values of input shear stress (τ) should be used. Further research should be performed to estimate the correction factor in determining the values of τ .

7.5 Conclusions

- The amplification ratio relationship as proposed by Seed and Idriss (1982) overestimates the values of a_{\max} obtained from FLAC analyses.
- The cases with Loma Prieta earthquake de-amplify the input acceleration time history (pga) while it is amplified for cases with Saguenay earthquake, except for cases with the presence of soft clay underlying the silty sand layer.
- The use of aggregate pier amplifies the ground acceleration (a_{\max}) by a factor ranges from 1.55 to 3.13 for the Loma Prieta earthquake and 1.04 to 1.67 for the Saguenay earthquake. The average value for both earthquakes ranges from 1.4 to 2.3. This phenomenon agrees to findings by other researchers, for example by Liu and Dobry (1997) and by Mitchell, et al. (1998).
- For Loma Prieta earthquake the frequency of pga coincides with the frequencies of a_{\max} . For Saguenay earthquake the frequency of pga is slightly larger than the frequencies of a_{\max} . It can also be concluded that cases using Loma Prieta earthquake generally show spectra with

low frequency (high period) while cases using Saguenay earthquake generally show spectra with high frequency (low period).

- For Loma Prieta earthquake most r_u values increase due to the installation of aggregate pier. On the contrary, most r_u values decrease due to the installation of aggregate pier for Saguenay earthquake. Therefore, improvement is much more significant in cases with Saguenay earthquake time history. It can be concluded that generally improvement occurs due to the installation of aggregate pier.
- The residual (steady state) r_u values calculated using Marcuson, et al. (1990) procedure underestimate those calculated using FLAC.
- The values of r_d calculated by using the values of τ_{max} from FLAC show a relatively narrow range with values for case without aggregate pier are generally larger than those of case with aggregate pier. The values of r_d calculated using FLAC are generally less than those proposed by the Simplified Procedure (Seed and Idriss, 1971).
- The values of K_G as proposed by Baez and Martin (1993, 1994) and Goughnour and Pestana (1998) can be estimated by applying values of τ_{max} calculated using FLAC. It can be concluded that the K_G values in the aggregate pier are larger than those in the soil matrix. This shows that the installation of aggregate pier is effective in that the aggregate pier carries more shear stresses than the soil matrix under seismic loading.
- A modification to the shear stress reduction factor (K_G) was introduced that is the shear stress reduction factor, which takes into account the reinforcement factor (K_{GR}), which is defined as the ratio of the maximum shear stress for case with aggregate pier to that of case without aggregate pier obtained from FLAC analyses. The K_{GR} values in the aggregate pier are much larger than those in the soil matrix. This again shows that the aggregate pier carries more shear stresses than the soil matrix under seismic loading.
- The value of K_G calculated based on shear stresses from FLAC normalized by those from the Simplified Procedure is smaller than the value of K_{GR} . The use of K_{GR} value is more preferable since it depicts the “real” reinforcing effects of aggregate pier. It can be concluded that the use of K_G overestimates the reduction in shear stress of soil matrix during seismic loading compared to the use of K_{GR} . It should be noted, however, that the low K_G values reflect the uncertainty of the shear stresses calculated by the Simplified Procedure (Seed and Idriss, 1971).

- A simple procedure was developed to estimate the value of K_{GR} . It was found that the equation proposed by Baez and Martin (1993, 1994) agrees well with the value of K_{GR} calculated using FLAC. The equation proposed by Goughnour and Pestana (1998) overestimates the value of K_{GR} .
- The results from FLAC analyses seem contradict with those from the Simplified Procedure (Seed and Idriss, 1971) in terms of estimating the values of r_d and K_G . It is recommended to use the values of K_{GR} estimated using equation proposed by Baez and Martin (1993, 1994).
- A simple design procedure was proposed to estimate the shear stress in the soil matrix (τ_s) under seismic loading. This procedure should be used with judgment as to which values of input shear stress (τ) should be used. Further research should be performed to estimate the correction factor in determining the values of τ .

Table 7.1 Frequency at which peak ground acceleration occurs (Loma Prieta earthquake)

Condition	Case no.	a_{max} (g)	Frequency (Hz)
Input pga	Loma Prieta	0.45	1.42
No aggregate pier	1C	0.16	1.60
	3C	0.16	1.56
	5C	0.13	1.42
	7C	0.27	1.44
With aggregate pier	2C	0.38	2.71
	4C	0.38	1.71
	6C	0.42	1.42
	8C	0.42	1.44
	9C	0.43	1.42

Table 7.2 Frequency at which peak ground acceleration occurs (Saguenay earthquake)

Condition	Case no.	a_{max} (g)	Frequency (Hz)
Input pga	Saguenay	0.050	11.98
No aggregate pier	1S	0.086	8.04
	3S	0.059	8.04
	5S	0.038	3.98
	7S	0.056	4.27
With aggregate pier	2S	0.100	8.37
	4S	0.098	8.36
	6S	0.040	6.47
	8S	0.062	4.27
	9S	0.099	8.37

Table 7.3 Comparison of r_u values (steady state) between Seed-Idriss (1971) and Marcuson-Hynes-Franklin (1990) and FLAC

Depths	Case 1S			Case 3S		
	FS (SI)	r_u (MHF)	r_u (FLAC)	FS (SI)	r_u (MHF)	r_u (FLAC)
Point 1 (2.25 ft)	2.57	0 to 0.0602	0.87	3.76	0 to 0.0232	0.92
Point 2 (4.75 ft)	2.58	0 to 0.0596	0.65	3.78	0 to 0.0229	0.57
Point 3 (9.75 ft)	2.61	0 to 0.0579	0.33	3.82	0 to 0.0223	0.26
Point 4 (12.25 ft)	2.63	0 to 0.0568	0.24	3.85	0 to 0.0219	0.17
Point 5 (16.75 ft)	N/A	N/A	N/A	3.89	0 to 0.0213	0.091
Point 6 (19.75 ft)	N/A	N/A	N/A	3.92	0 to 0.0209	0.08
Point 7 (24.25 ft)	N/A	N/A	N/A	3.96	0 to 0.0204	0.085

(Note: SI indicates Seed-Idriss, 1971 and MHF indicates Marcuson-Hynes-Franklin, 1990)

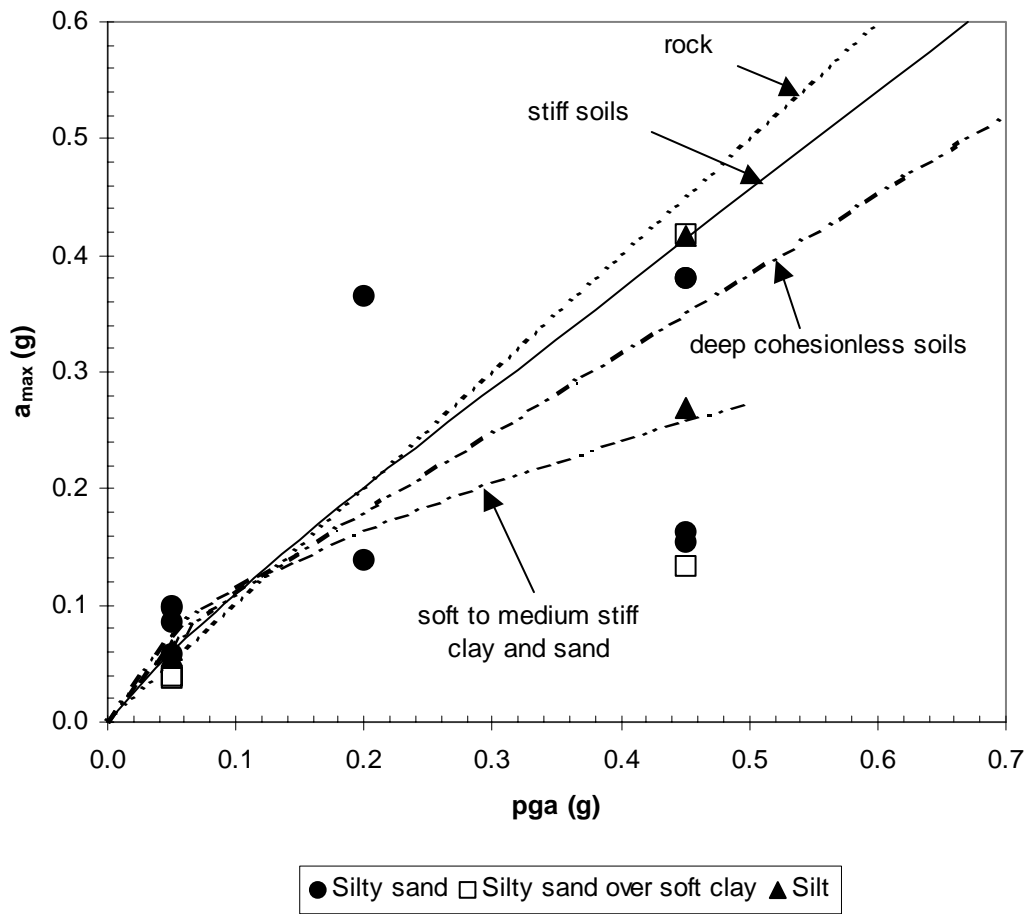


Figure 7.1 Plot of amplification ratios based on the soil type compared to those proposed by Seed and Idriss (1982)

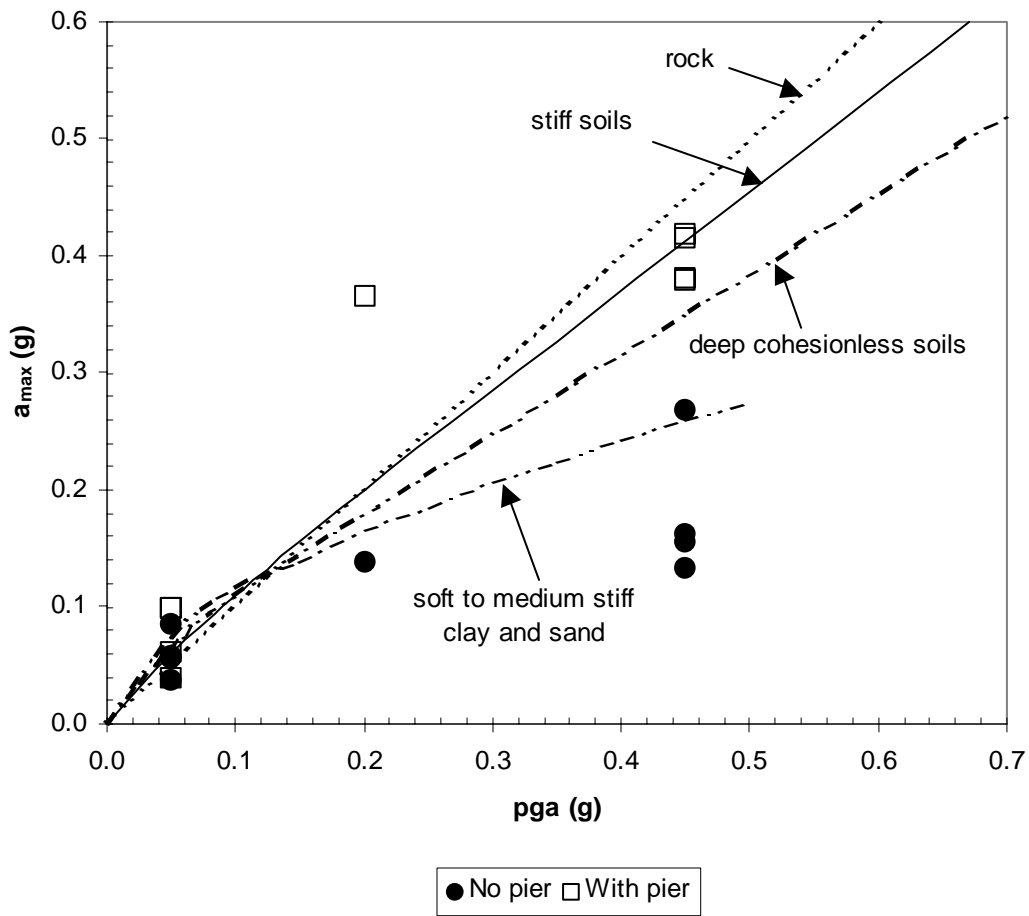


Figure 7.2 Plot of amplification ratios based on condition with and without aggregate pier compared to those proposed by Seed and Idriss (1982)

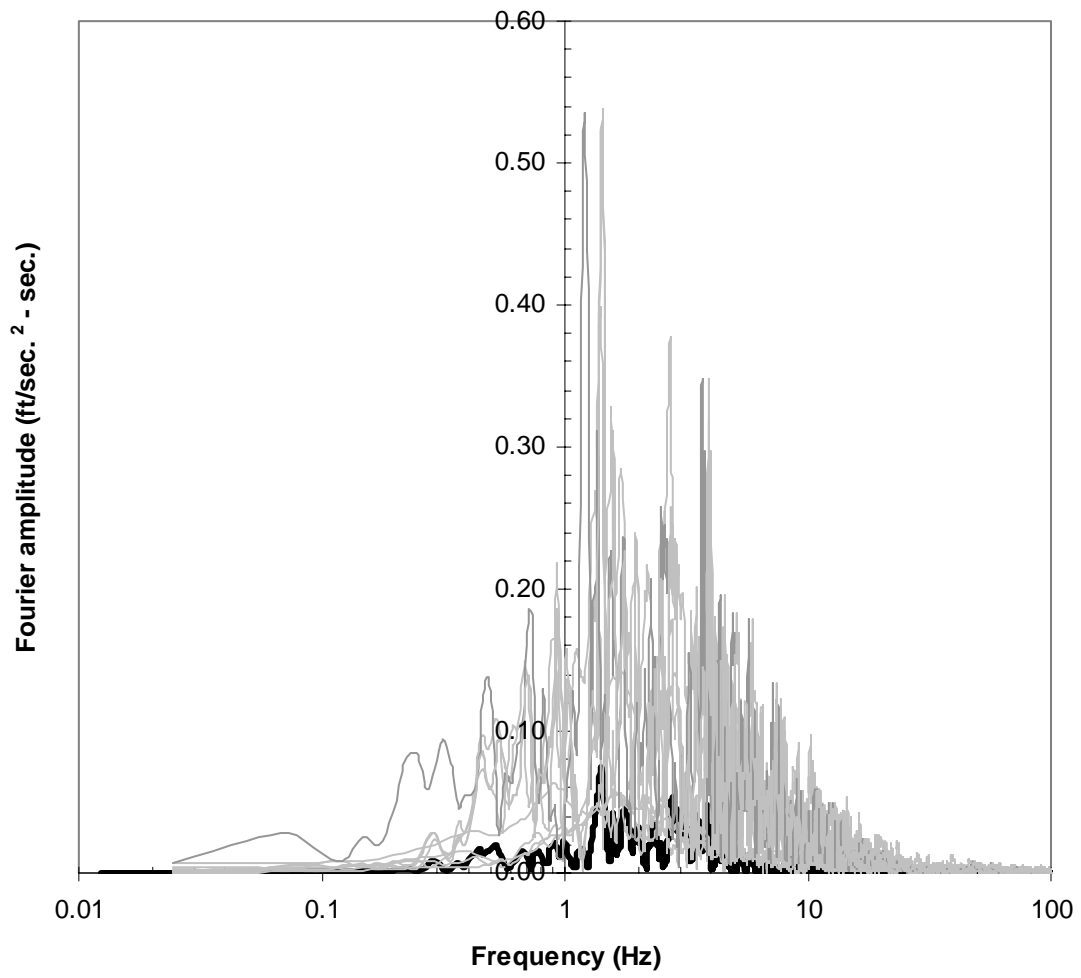


Figure 7.3 Fourier amplitude spectra for cases using Loma Prieta earthquake

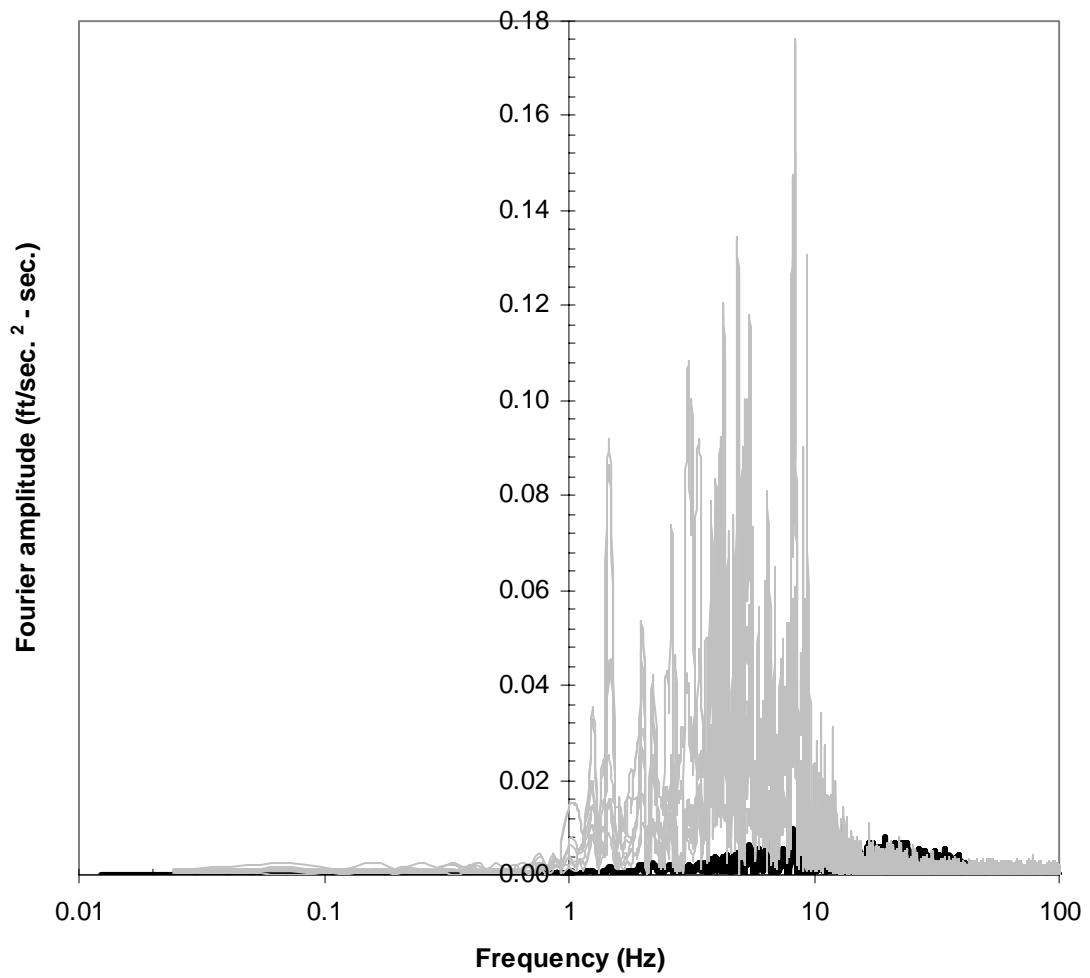


Figure 7.4 Fourier amplitude spectra for cases using Saguenay earthquake

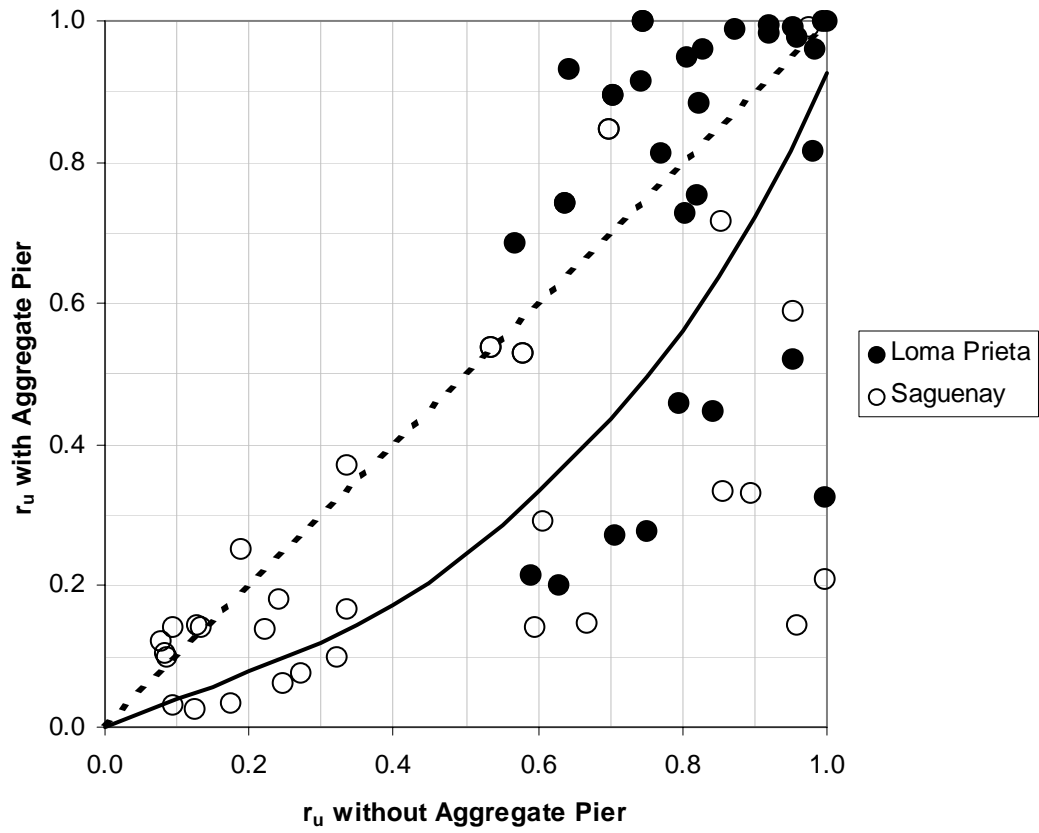


Figure 7.5 Comparison of peak values of r_u between cases with and without aggregate pier – Loma Prieta and Saguenay earthquakes

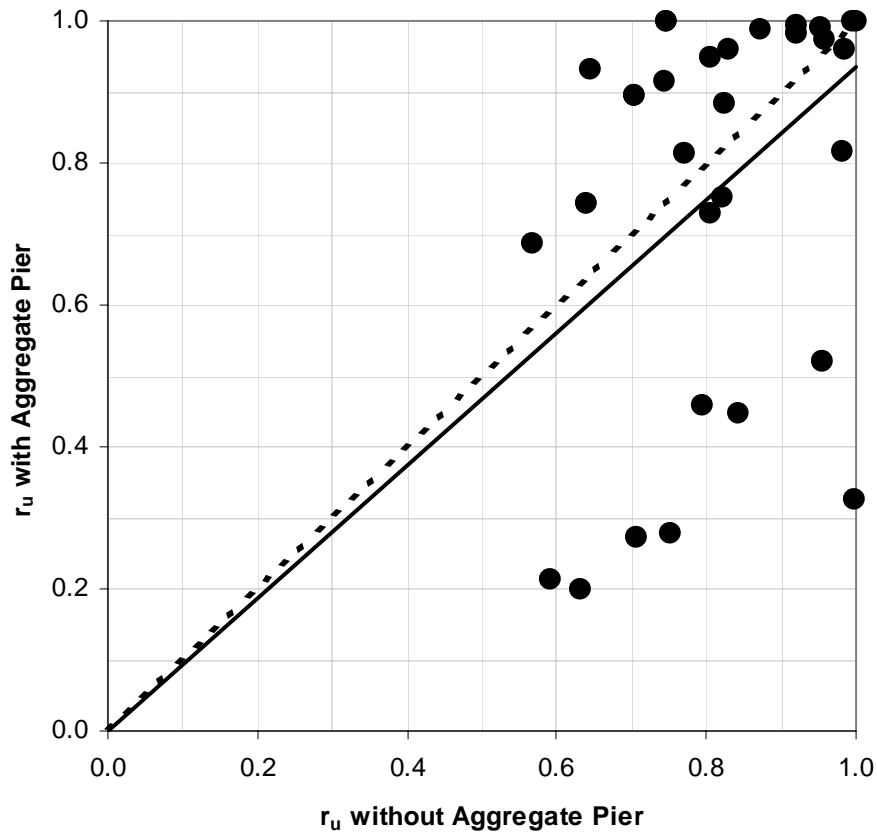


Figure 7.6 Comparison of peak values of r_u between cases with and without aggregate pier – Loma Prieta earthquake

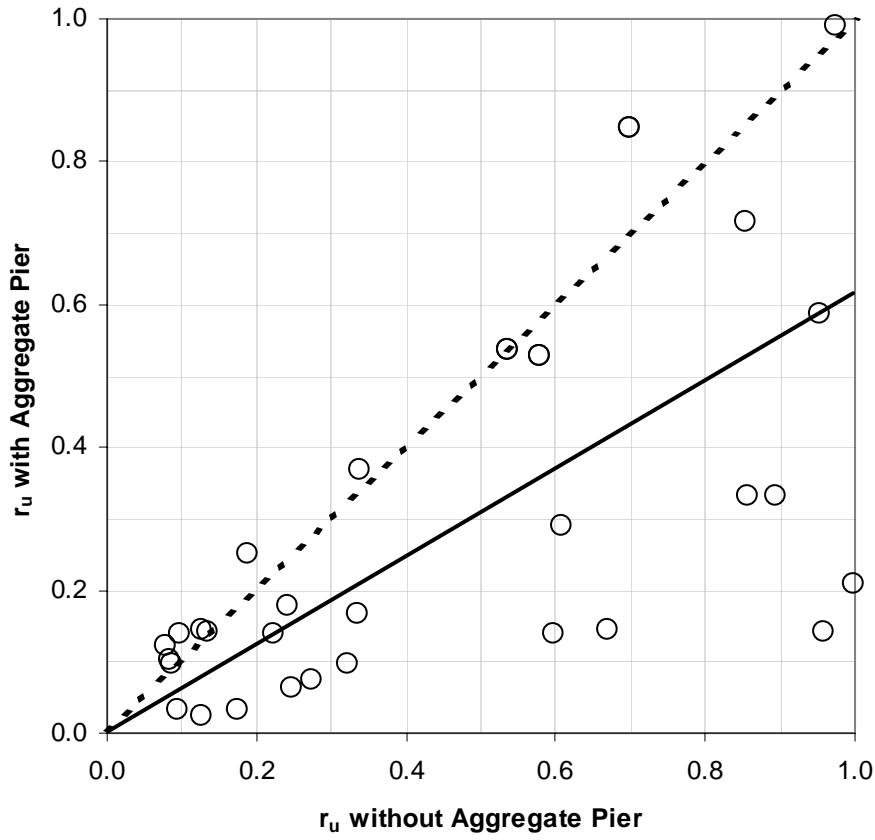


Figure 7.7 Comparison of peak values of r_u between cases with and without aggregate pier – Saguenay earthquake

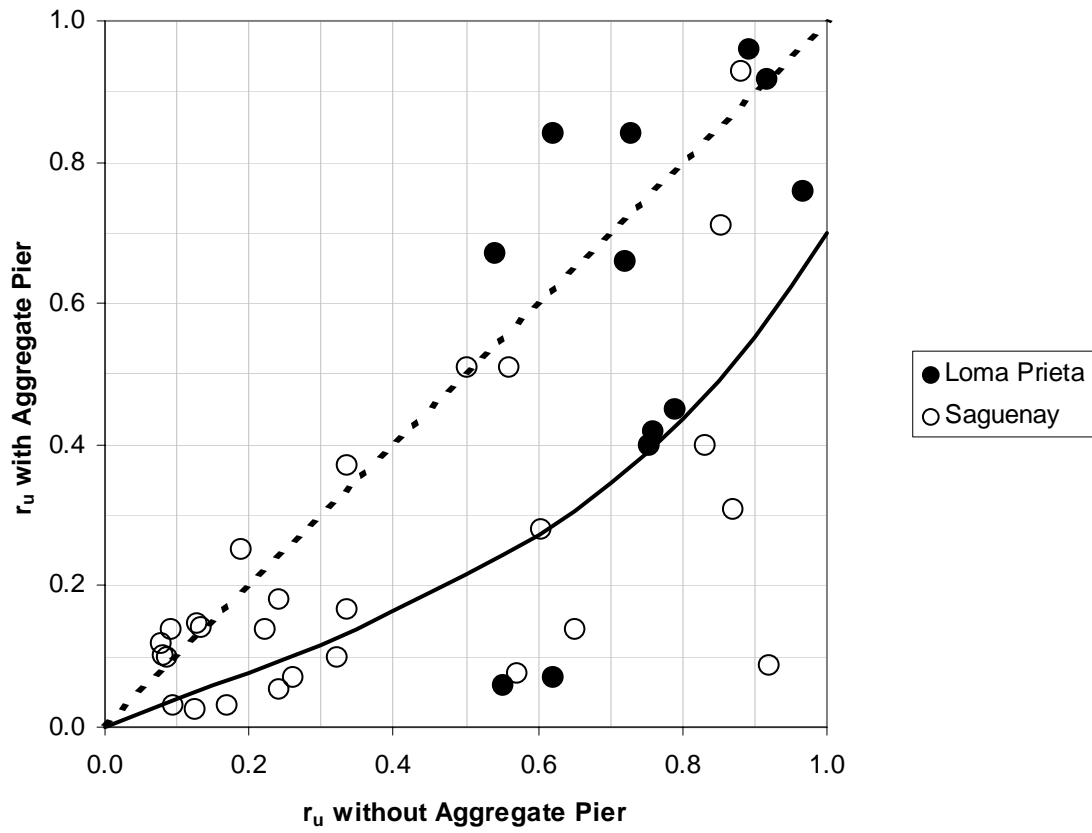


Figure 7.8 Comparison of steady state values of r_u between cases with and without aggregate pier (Loma Prieta and Saguenay earthquakes)

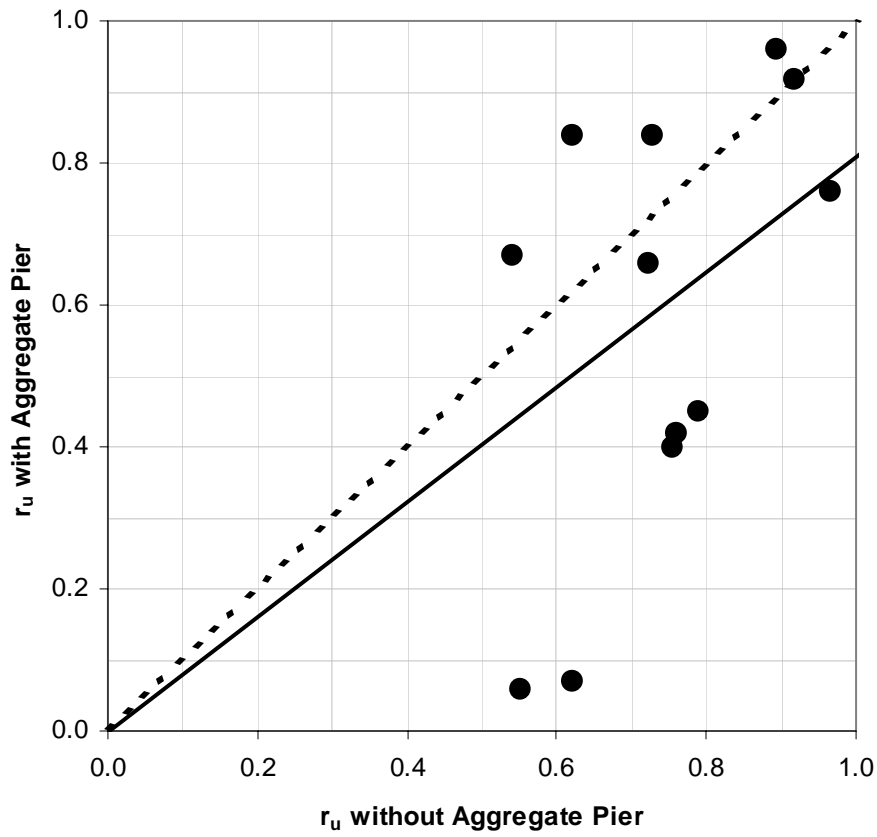


Figure 7.9 Comparison of steady state values of r_u between cases with and without aggregate pier (Loma Prieta earthquake)

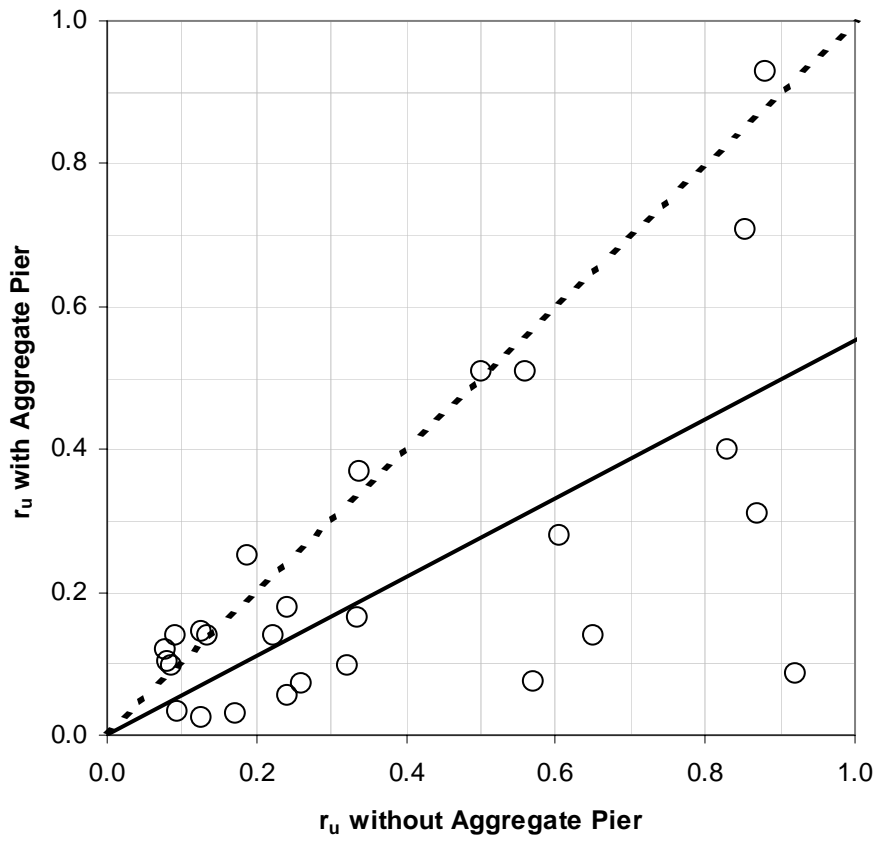


Figure 7.10 Comparison of steady state values of r_u between cases with and without aggregate pier (Saguenay earthquake)

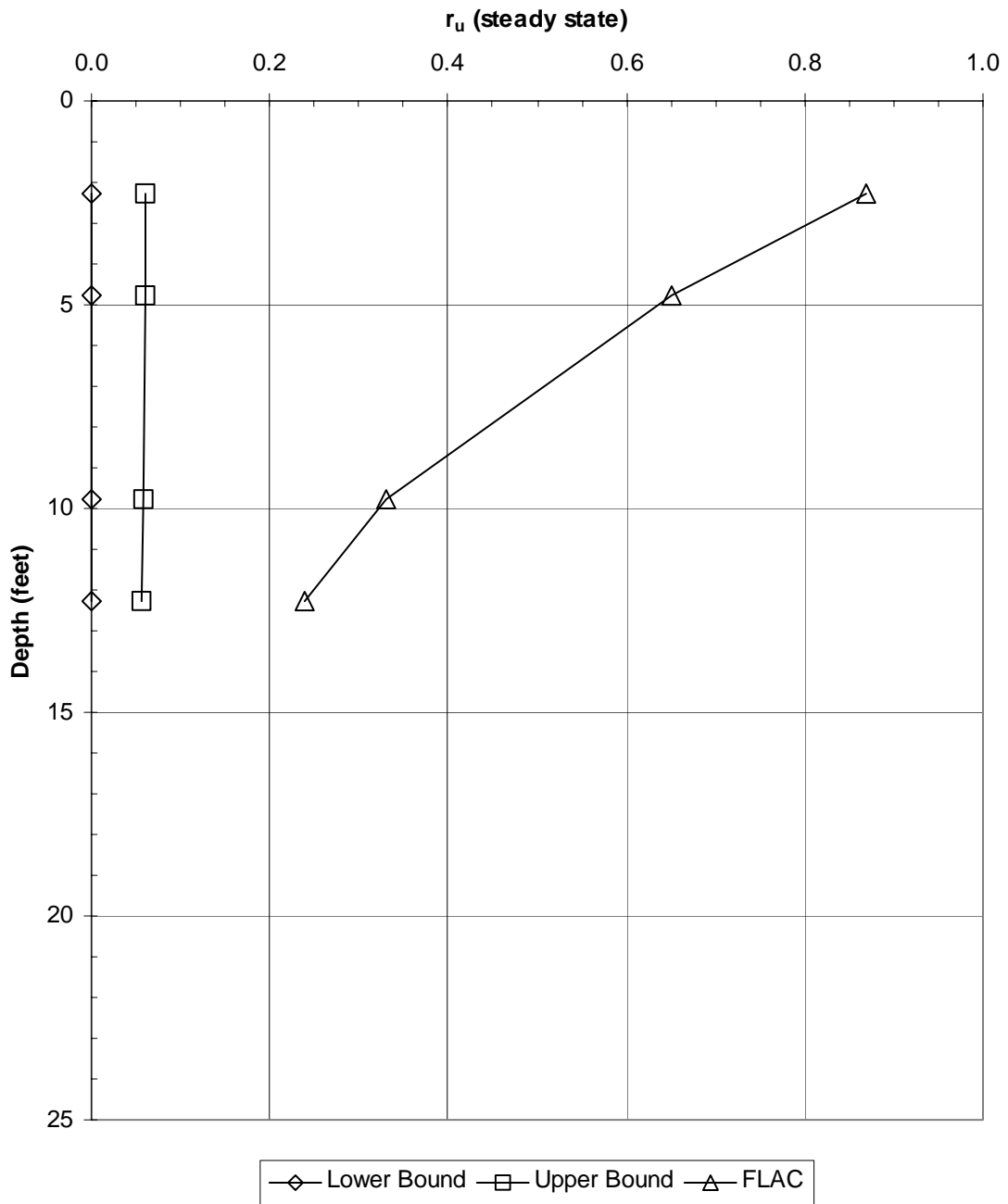


Figure 7.11 Comparison of r_u values between SI & MHF and FLAC for Case 1S
 (Note: SI indicates Seed-Idriss, 1971 and MHF indicates Marcuson-Hynes-Franklin, 1990)

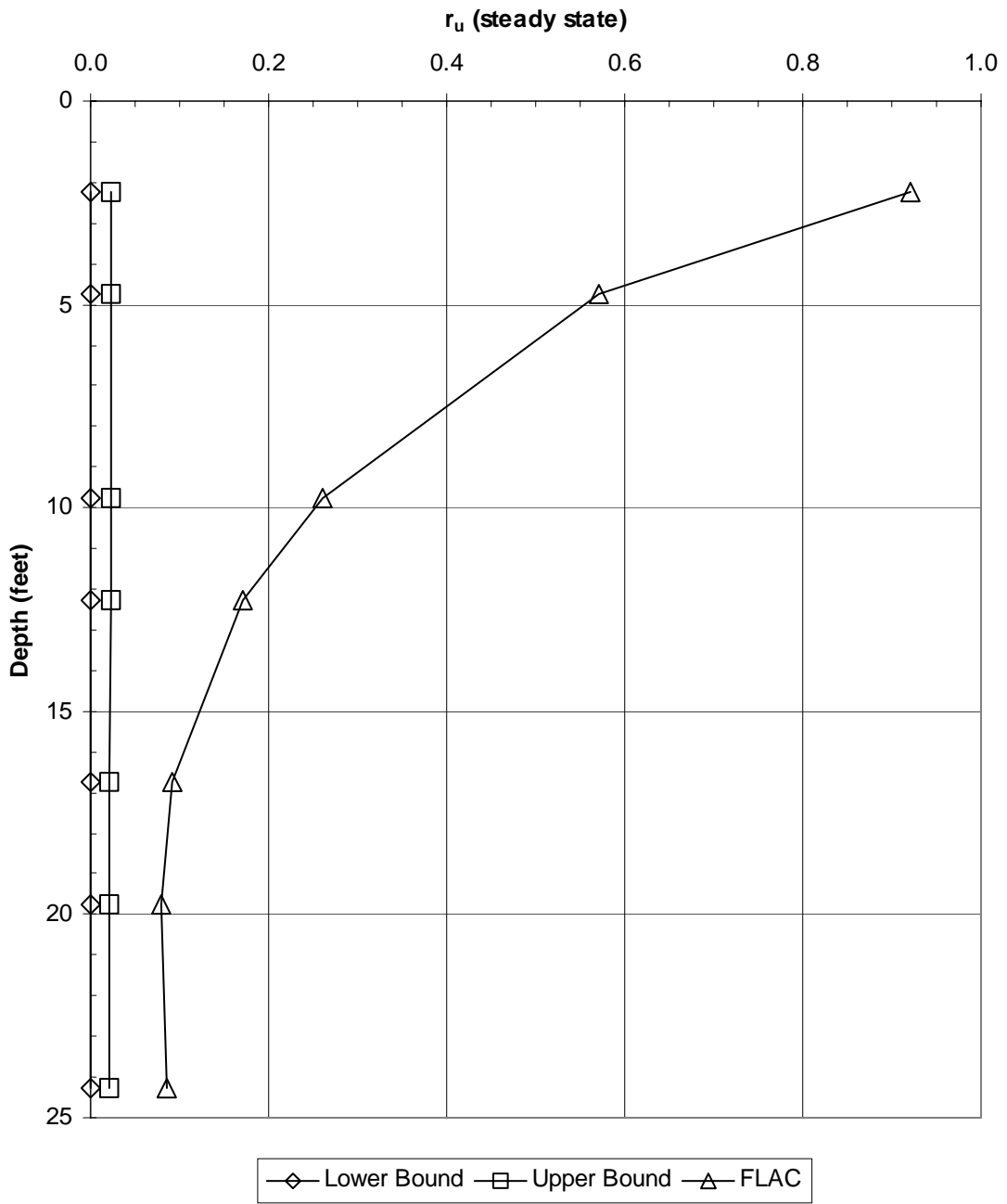


Figure 7.12 Comparison of r_u values between SI & MHF and FLAC for Case 3S

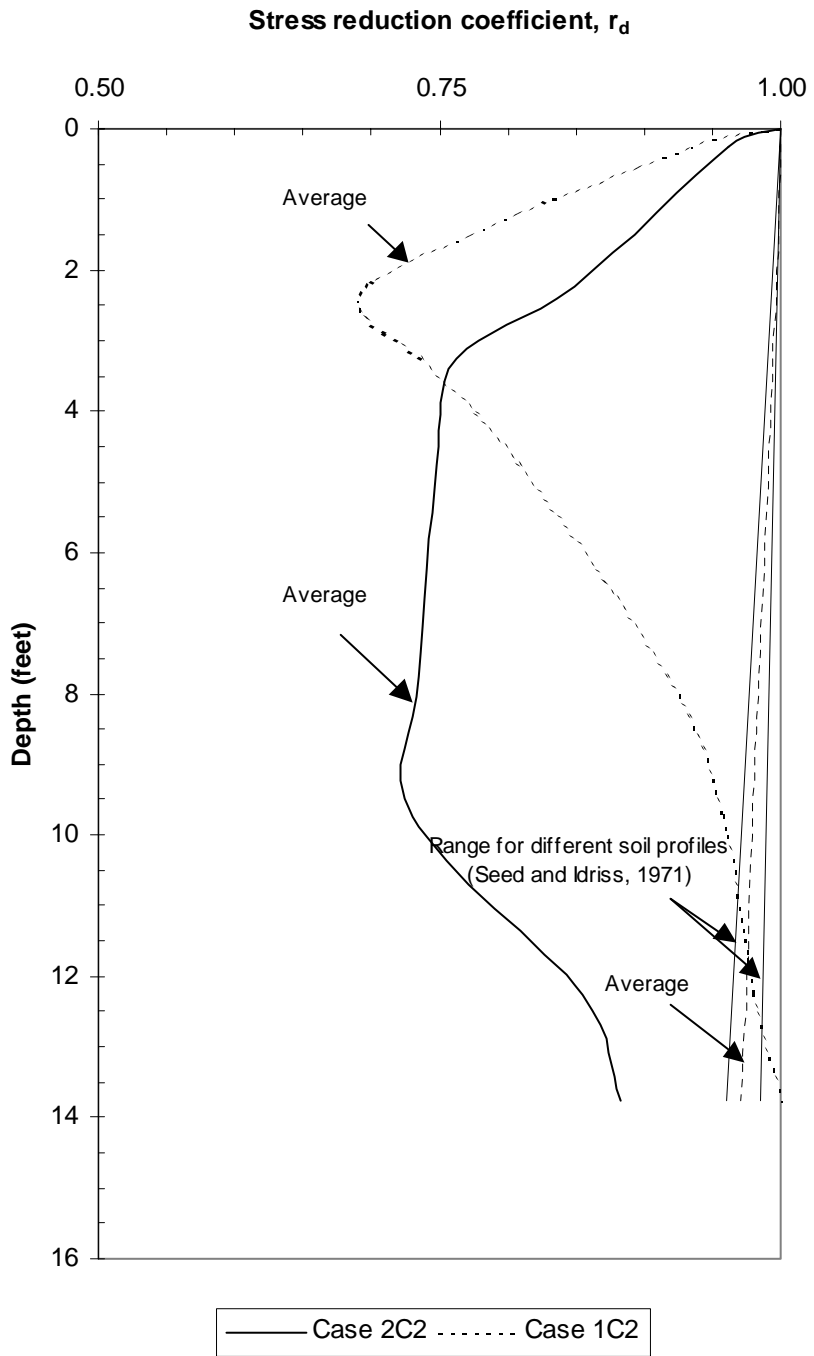


Figure 7.13 Stress reduction coefficient (r_d) for Cases 1C2 and 2C2

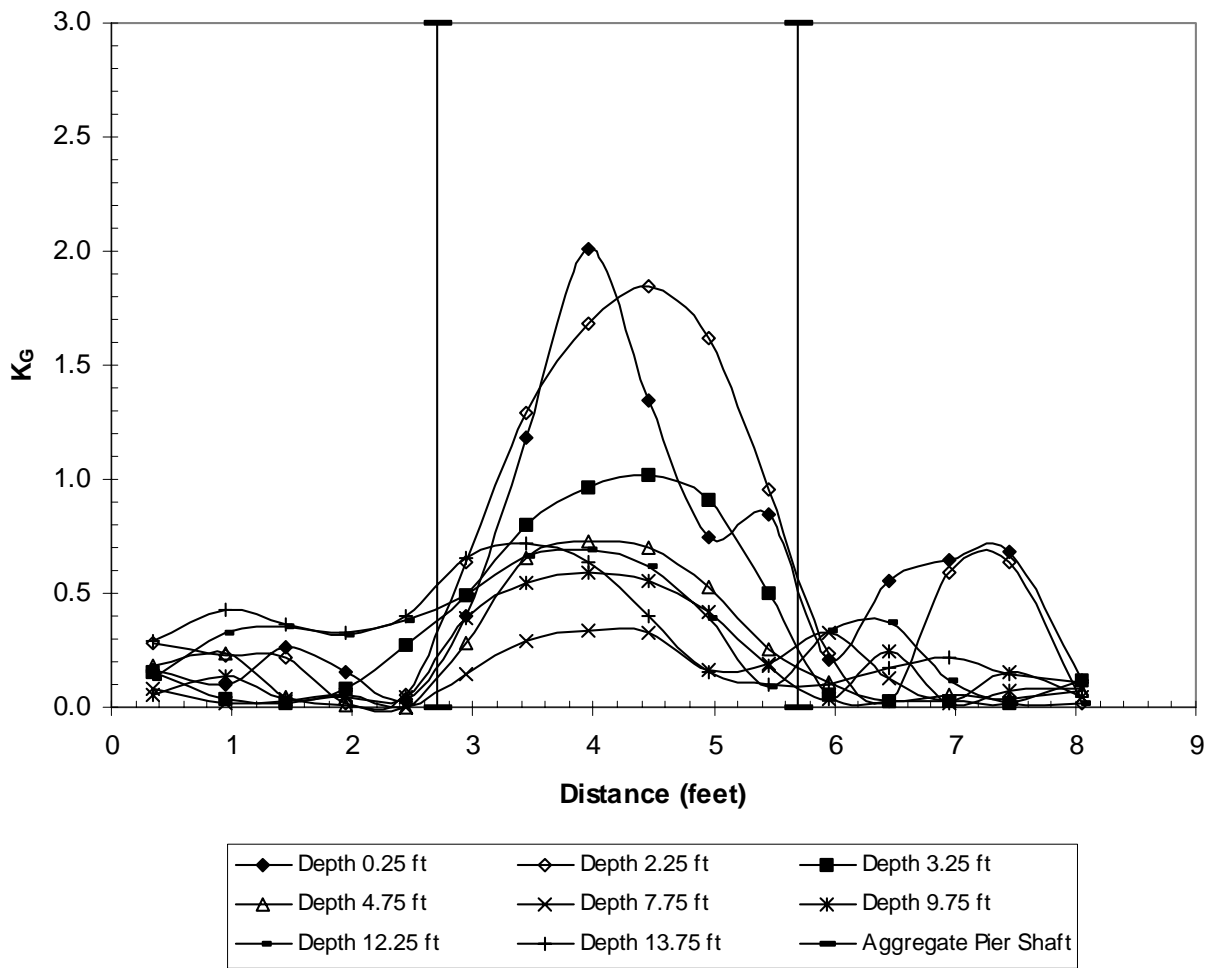


Figure 7.14 Plot of values of K_G versus distance for different depths for Case 2C2

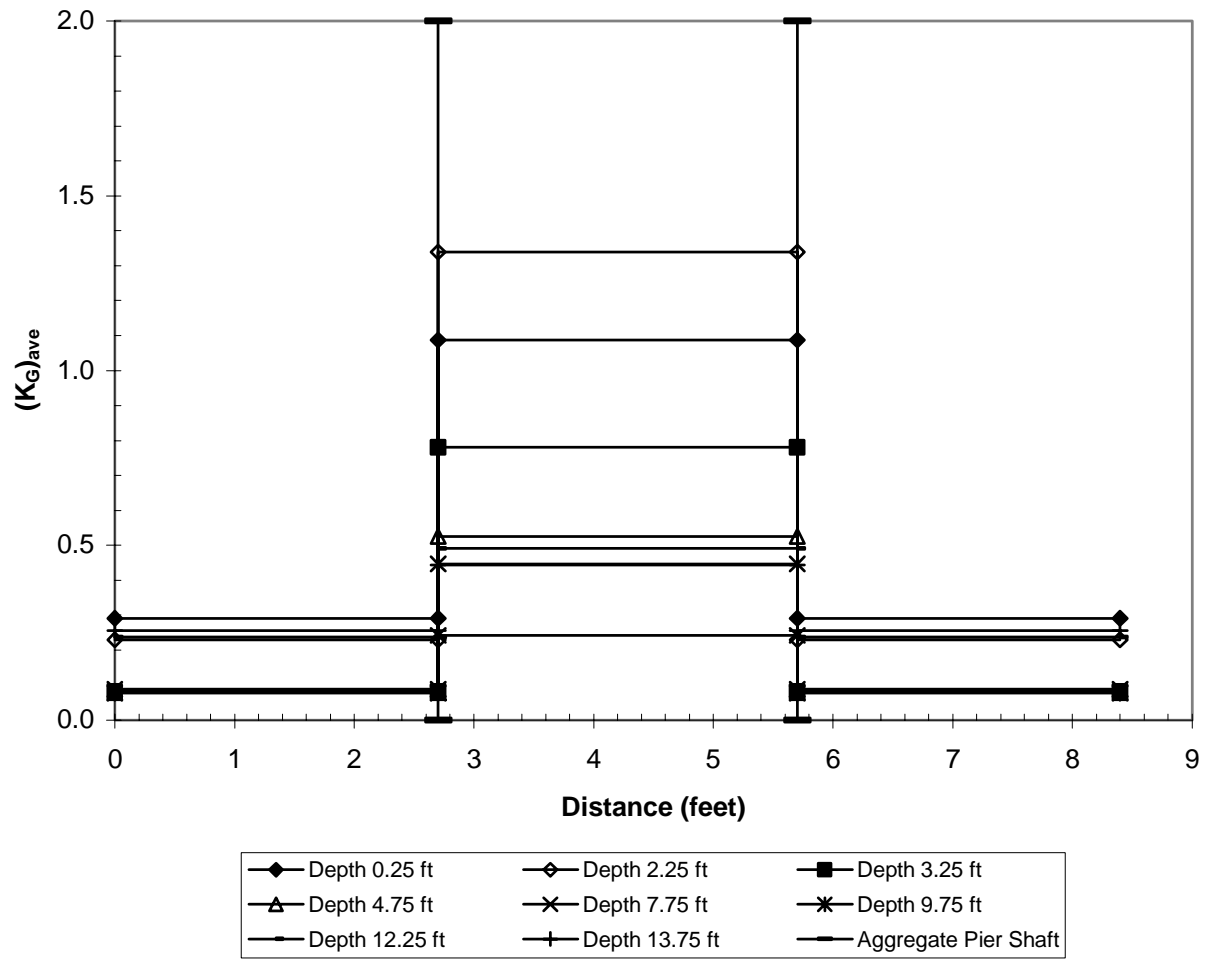


Figure 7.15 Plot of values of $(K_G)_{ave}$ versus distance for different depths for Case 2C2

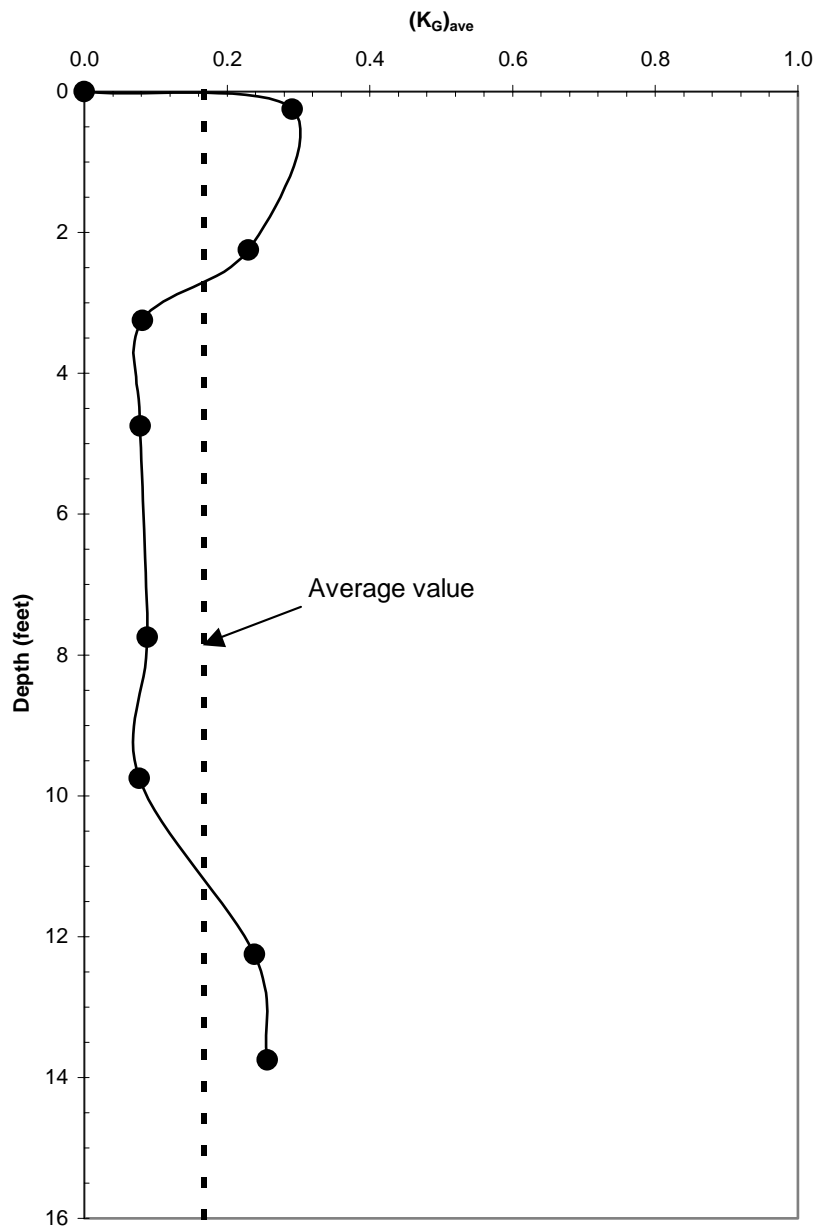


Figure 7.16 Plot of values of $(K_G)_{ave}$ versus depths for Case 2C2

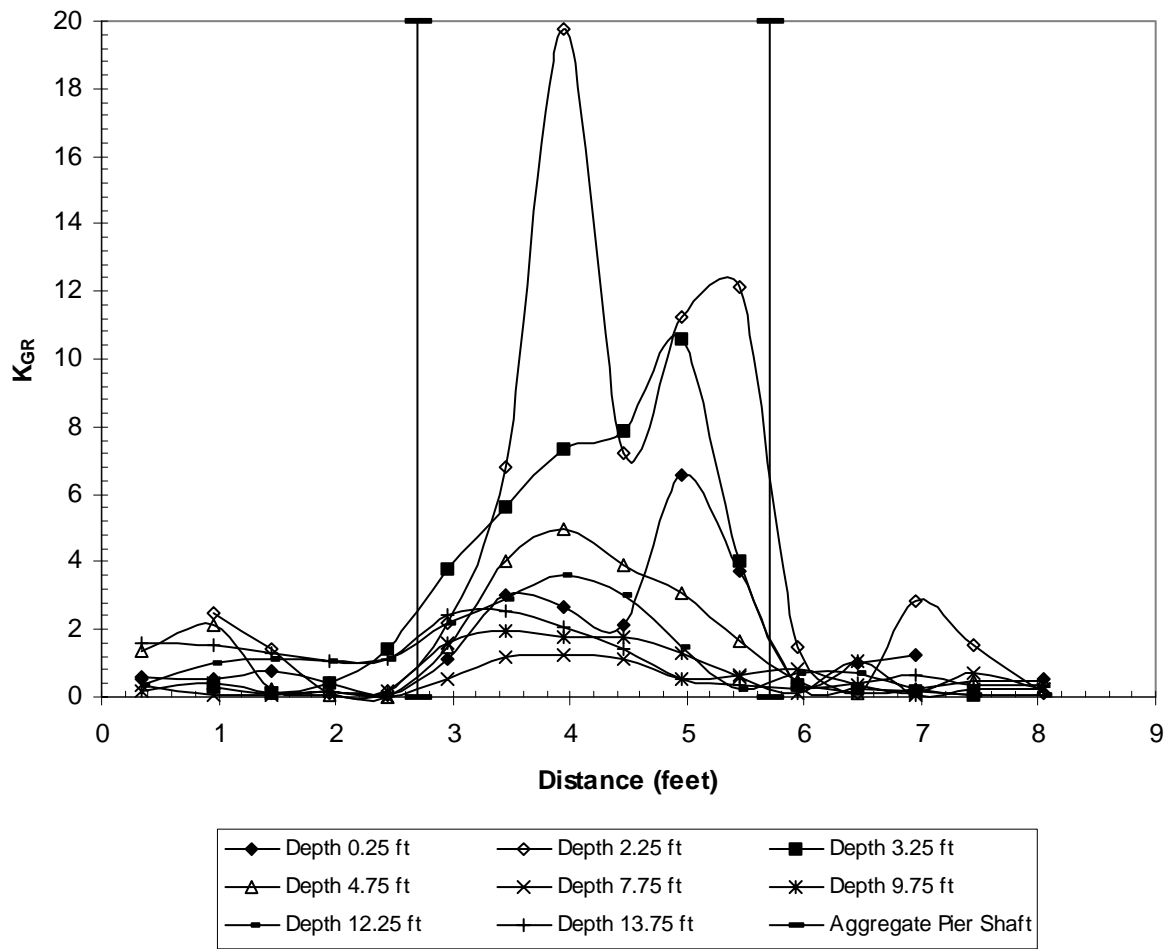


Figure 7.17 Plot of values of K_{GR} versus distance for different depths for Case C2

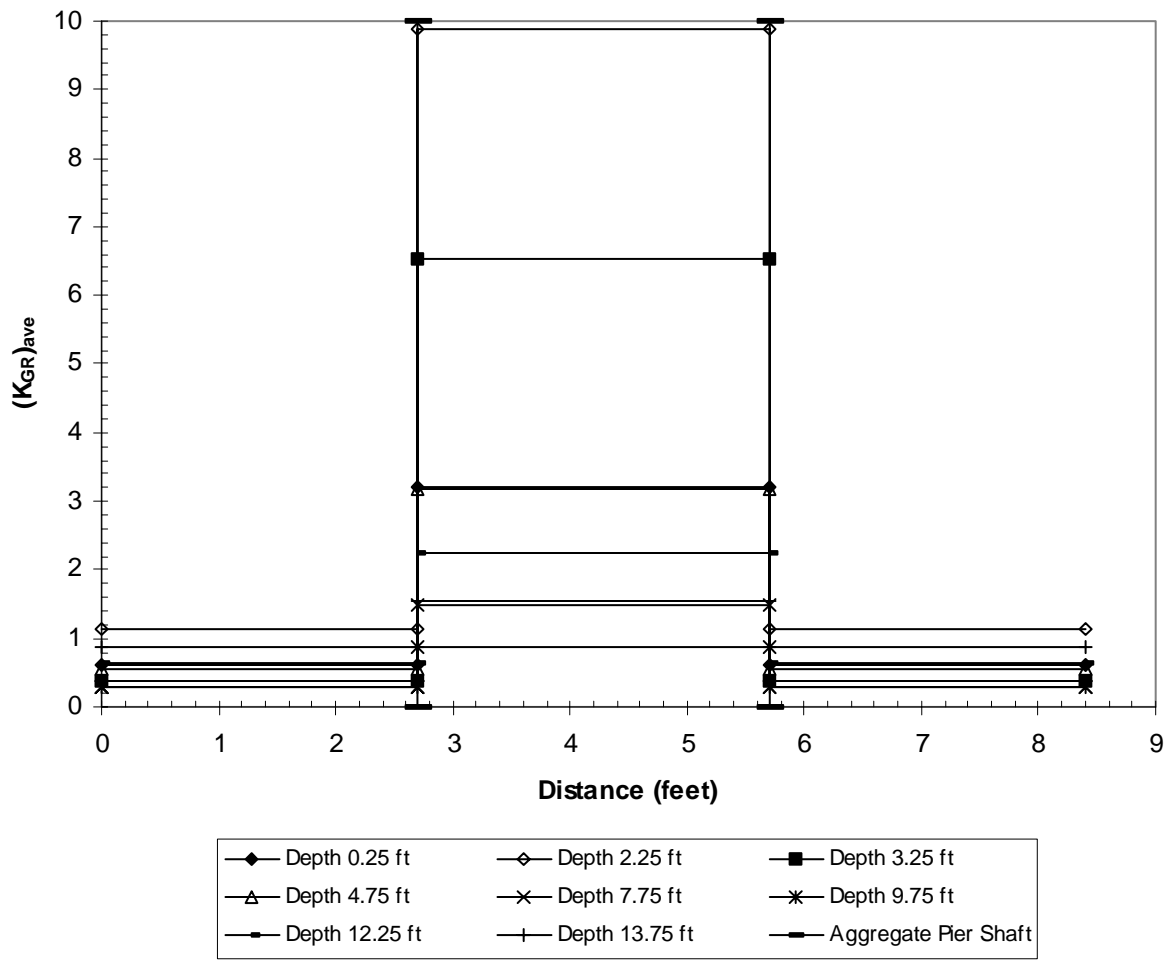


Figure 7.18 Plot of values of $(K_{GR})_{ave}$ versus distance for different depths for Case C2

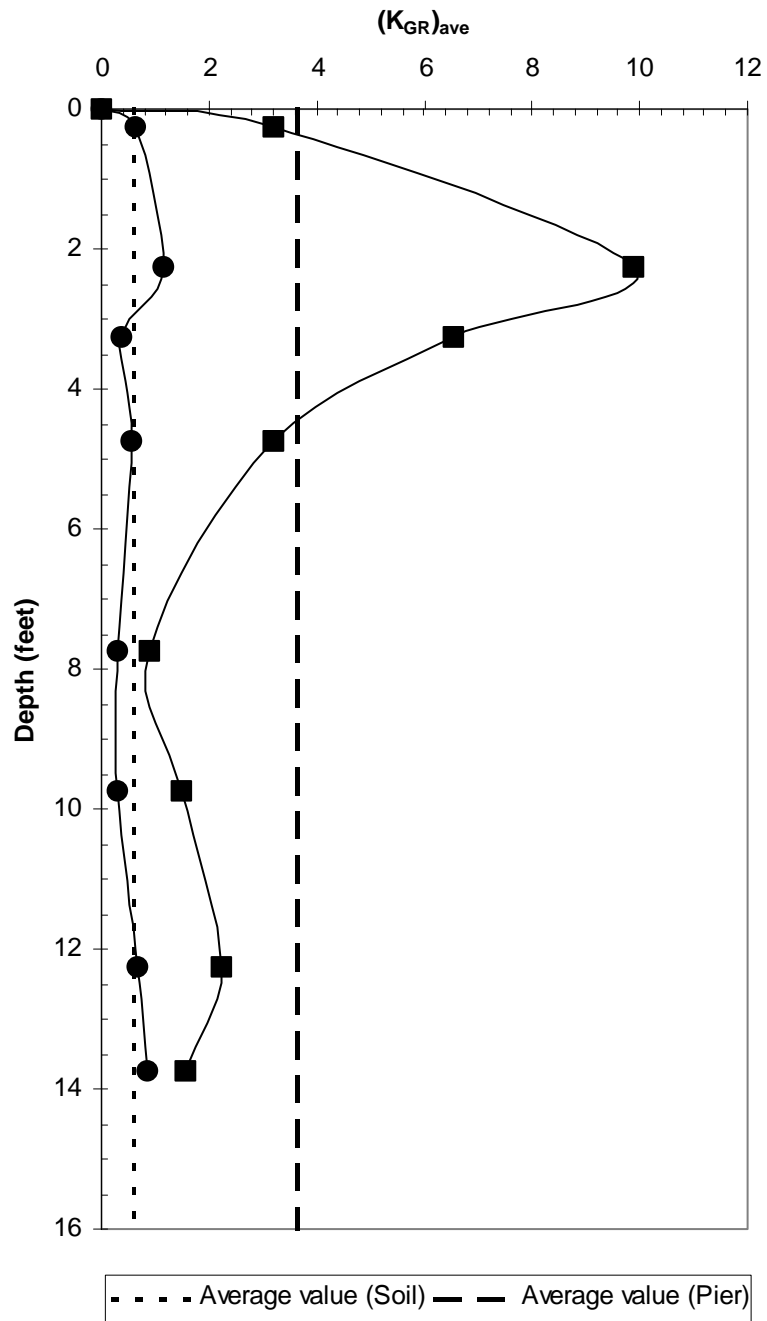


Figure 7.19 Plot of values of $(K_{GR})_{ave}$ versus depths for Case C2

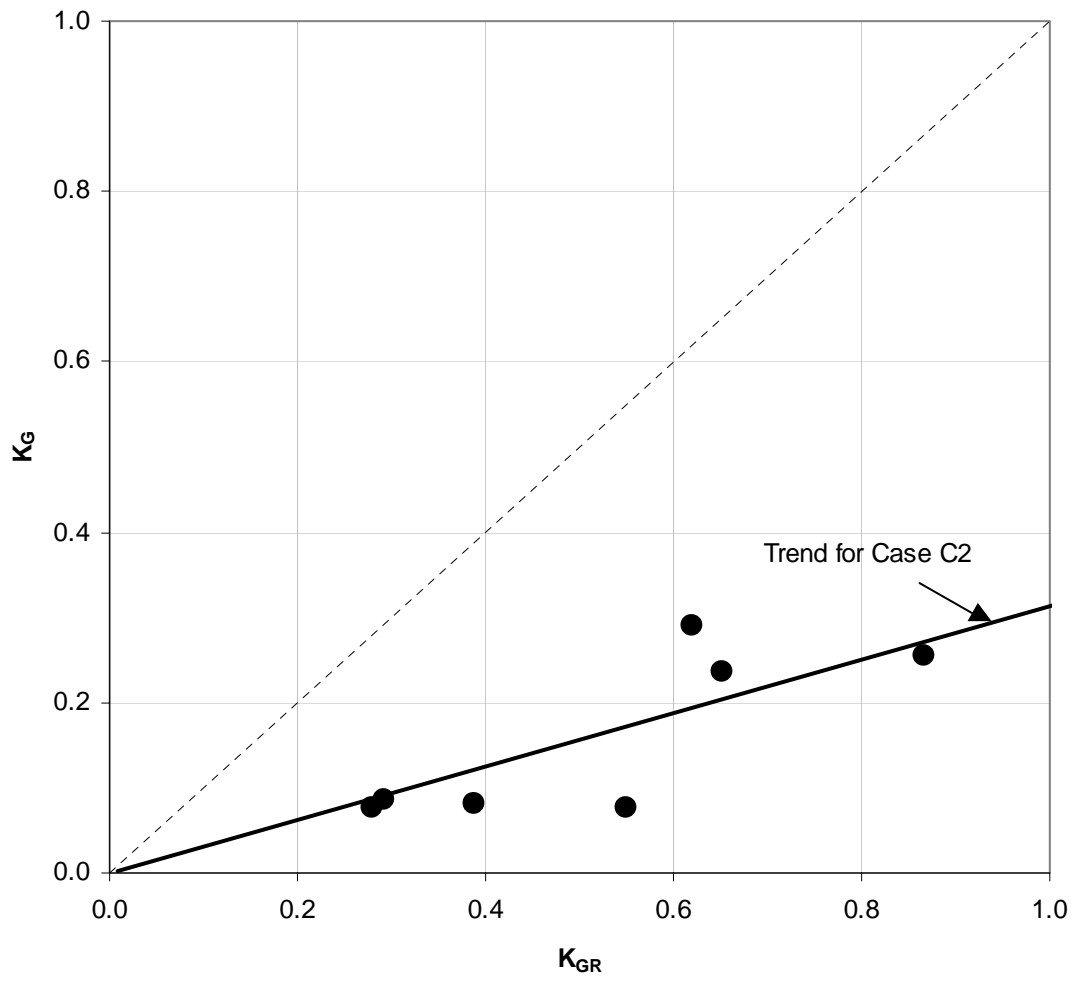


Figure 7.20 Comparison of values of K_{GR} and K_G in the soil matrix at various depths for Case C2

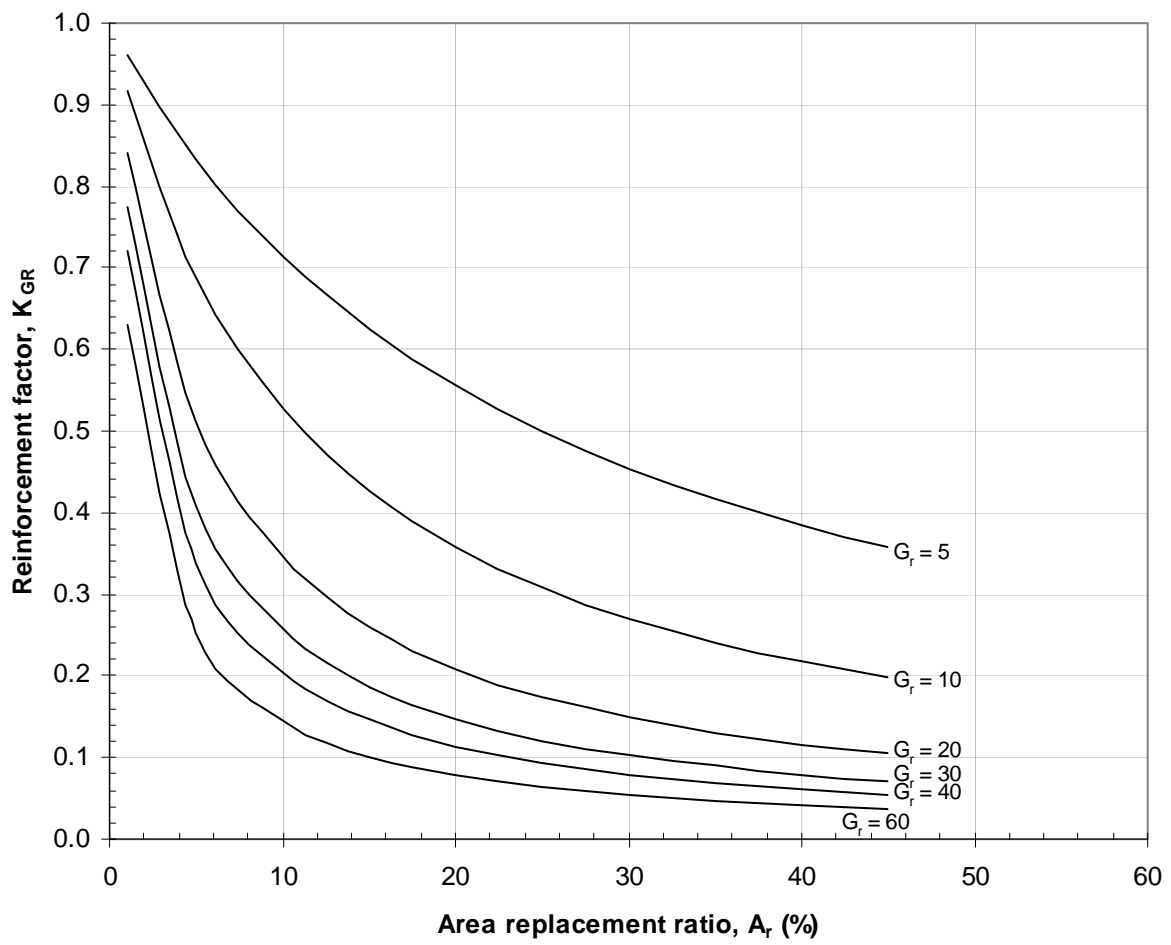


Figure 7.21 The reinforcement factor, K_{GR} (after Baez and Martin, 1993, 1994)

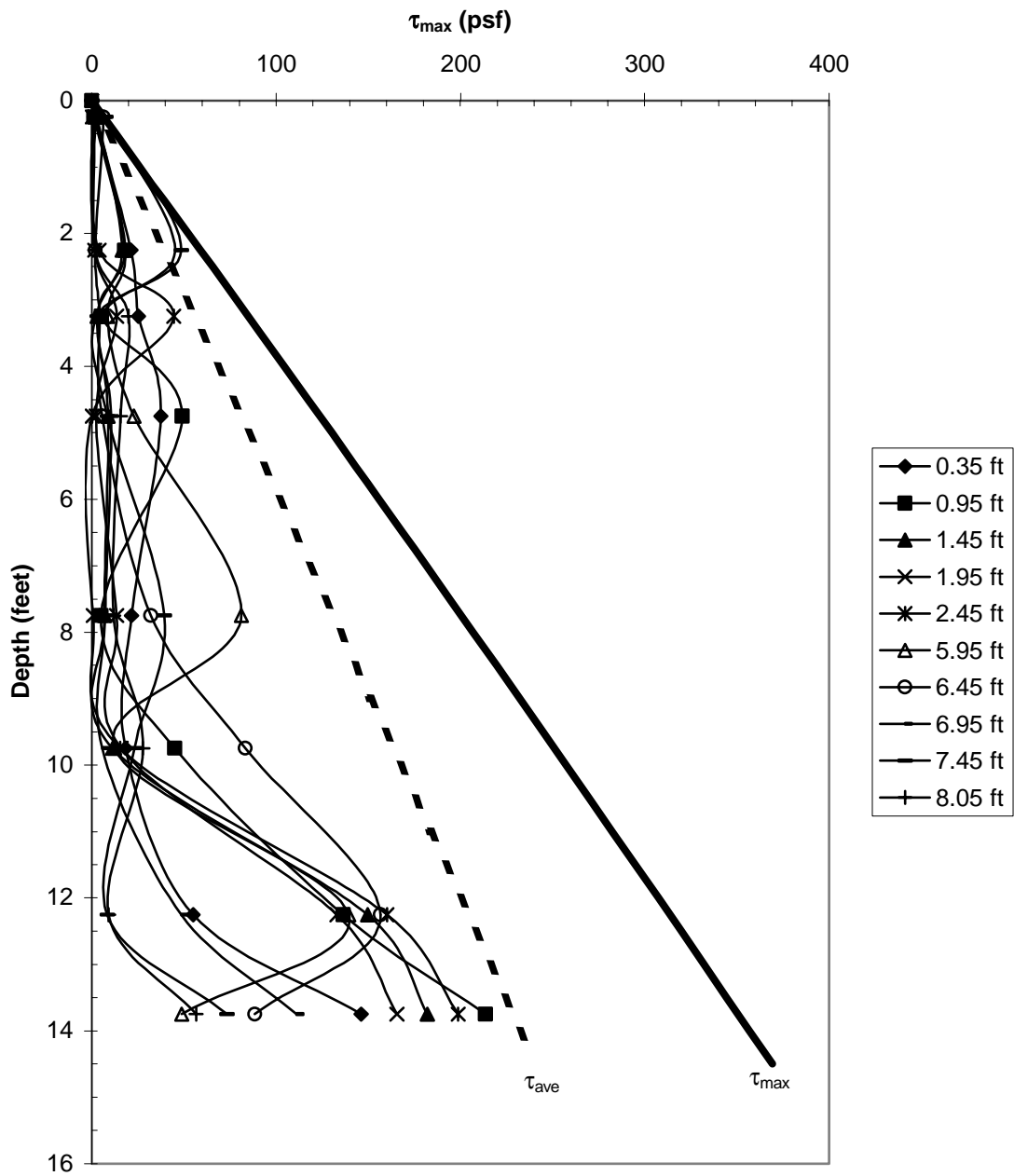


Figure 7.22 Estimation of shear stresses in soil matrix using K_{GR} for Case 2C2